Energy performance of self-powered Green IoT nodes

Godlove Suila Kuaban [1,*], Tadeusz Czachórski [1], Erol Gelenbe [1], Sapana Sharma [2], Pradeep Singh [2], Piotr Pecka [1], Valery Nkemeni [3], and Piotr Czekalski [4]

[1] *Institute of Theoretical and Applied informatics, Polish Academy of Sciences (IITiS-PAN), Baltycka 5, Gliwice, Poland*
[2] *Department of Mathematics, MMEC, Maharishi Markandeshwar (Deemed to be University) Mullana, Haryana-133203, India*
[3] *Laboratory of Electrical Engineering and Computing, Faculty of Engineering and Technology, University of Buea, P.O.Box 63, Buea, Cameroon*
[4] *Faculty of Automatic Control, Electronic, and Informatics, Silesian University of Technology Gliwice, Poland*

Correspondence*:
Godlove Suila Kuaban
gskuaban@iitis.pl

ABSTRACT

The widespread adoption of the Internet of Things (IoT) partly depends on the successful design and deployment of IoT nodes that can operate for several years without any service outage and the need to replace their energy storage systems (e.g., battery, capacitor, or supercapacitor) when all the stored energy is depleted or when the cycle life of the Energy Storage Systems (ESS) is reached. Replacing batteries in the case of large-scale IoT networks and nodes located in places that are hard to reach is very challenging and costly, requiring the design of IoT nodes that can operate for several years without the need for human intervention. One such example is the deployment of IoT nodes in large agricultural fields (for soil or crop monitoring) or a long-distance pipeline (for pipeline monitoring). This paper investigates the practical implications of imposing energy-saving thresholds on the energy performance metrics of green IoT nodes. We propose an energy packet-based model for the evaluation of the energy performance of a green IoT node with the possibility of switching the node to energy saving regimes on the fly when the energy content of the ESS reaches defined thresholds. Configuring single or multiple thresholds improves the energy performance of the node significantly (e.g., increases lifetime of the node, reduces probability of service outage and energy wastage), and the value of the threshold(s) should be carefully chosen.

Keywords: Energy performance, green IoT, energy packets, energy-efficiency, energy thresholds, time-dependent analysis.

1 INTRODUCTION

The widespread adoption of the Internet of Things (IoT) partly depends on the successful deployment of IoT nodes that can operate for several years without the need for battery replacement. In most IoT deployments, the IoT sensor/actuator nodes are powered by non-rechargeable batteries. A significant drawback of using non-rechargeable batteries is that the lifetime of the IoT network is limited by the finite energy capacity of their batteries Ku et al. (2015). Since energy depleted from the battery is not being replenished, the energy stored in the battery is eventually depleted, requiring the replacement of batteries, which is a costly operation and also very challenging in large-scale IoT networks and nodes located in locations that are hard to reach. For example, it is very challenging and costly to replace the batteries of IoT nodes deployed in large agricultural fields (for soil or crop monitoring) or a long-distance pipeline (for pipeline monitoring). Thus, there is a severe need to design and deploy IoT networks in such a way that the nodes can operate for several years before requiring battery replacements.

There is a growing interest in the adoption of green IoT design as a viable strategy to increase the lifetime of IoT nodes (the time required to deplete all the energy stored in the energy storage system of an IoT node), reduce the carbon footprint of IoT networks, and ensure environmental sustainability of IoT deployments. Green IoT Al-Ansi et al. (2021); Sadatdiynov et al. (2023); Alsharif et al. (2023a) is an IoT design framework that seeks to minimise the energy consumption from the manufacturing and operation of IoT systems with the aim of minimising the carbon footprint or pollutants (e.g., CO2, electronic wastes and other toxic substances) produced from the manufacturing, deployment, and operation of IoT systems including other IoT related infrastructures (e.g., edge computing, core networks, cloud computing, and operation, provisioning, and maintenance systems).

Green IoT design involves the development of strategies to minimise energy consumption and also the use of energy harvesters to harvest energy from ambient renewable energy sources to power IoT systems. Some green IoT design mechanisms to minimise energy consumption include duty cycling, reduction of packet size, transceiver optimisation, energy-ware routing, energy-efficient sensing (e.g., adaptive sensing), reduction of protocol overhead, voltage & frequency control Abdul-Qawy et al. (2020); Alsharif et al. (2023b) energy-efficient hardware and software design Albreem et al. (2021); Alsharif et al. (2023b), green IoT communication technologies (BLE, RFID, NFC, Zigbee, LoRa, Sigfox), green IoT architecture design (green cloud, fog, and virtualisation) Varjovi and Babaie (2020), sustainable materials, and integration of renewable energy into IoT systems. Also, the energy consumption of the IoT node can be reduced on the fly during its operation by throttling the speed of the processor clock, decreasing the operating voltage, or decreasing the transmission power(and the number of transmission operations).

The challenge in designing IoT nodes that can operate for several years without the need for battery replacement is the fact that the availability of ambient energy sources (e.g., light, wind, RF, heat, vibration, etc.) is random and sporadic, and the energy consumed by the nodes varies slightly. An approach for dimensioning Green IoT nodes without getting into the technical details of the energy harvesters, IoT nodes, and energy storage systems is to discretise energy into energy packets and apply well-known stochastic models such as Markov models. More details about the energy packet concept can be found in Gelenbe (2011, 2012); Kuaban et al. (2023a), and we have also presented more details about it in the next section, within the context of our proposed modelling framework.

A few studies (e.g.,Gautam and Dharmaraja (2018); Jones et al. (2011); Tunc and Akar (2017); Miao et al. (2023)) to analyse the energy performance of green IoT networks with the possibility of reducing the energy consumption of the node on the fly when the energy content of the ESS goes below-defined energy thresholds. In the analysis presented in most of these works, a single energy threshold is considered. Most of these works mostly focus on performance metrics such as the lifetime of the node. However, there are other performance metrics, such as service outage probability, the mean energy content of the ESS, and the energy wastage probability. There is also a need for more extensive investigation of the impact of the energy threshold on the energy performance metrics.

The main goal of this paper is to investigate the practical implications of imposing energy-saving thresholds on the energy performance metrics of green IoT nodes. We conduct steady-state and time-dependent analysis of the energy performance of a green IoT node, considering the impact of switching the node to more energy-efficient regimes when the defined threshold of the energy content of their ESS is reached. The main contributions of the paper include the following:

1. We propose an energy packet-based model for the evaluation of the energy performance of a green IoT node with the possibility of switching the node to more efficient regimes on the fly when the energy content of the ESS reaches defined thresholds.
2. We present an approach to determine the size of an energy packet or quantisation step that can be used to discretise or quantise the energy flows (energy harvested, stored, and consumed) into energy packets. In this way, energy is treated as the flow of discrete energy units (the so-called energy packets) rather than continuous flows.
3. We propose a multi-threshold model of the energy storage system and evaluated the impact of the value and number of thresholds on the energy performance metrics such as the service outage probability (the probability that all the energy packets stored in the ESS are depleted), energy wastage probability (the probability that ESS is full and energy packets that arrive after this time instant are lost or wasted), the mean number of energy packets in the ESS, and the lifetime of the ESS.

2 MODEL DESCRIPTION

In this section, we describe the energy model of a self-powered green IoT node considered in this paper. We also describe the energy packet model of the node and then use it to describe the energy threshold-based model of the energy storage system, which is the main focus of this paper.

2.1 Energy model of the self-powered IoT node

Consider a typical self-powered IoT node that consists of an IoT sensor node, an energy harvesting system, and an energy storage system, as shown in Fig. 1. Energy is harvested from ambient or external sources (e.g., solar, artificial light, Radio Frequency, and vibration) to power the sensor node directly. Any residual energy is stored in an energy storage system. The stored energy is used to power the sensor node when the energy harvester is not able to generate enough energy to meet the energy needs of the node due to unfavourable environmental conditions (e.g., during the night in the case of solar energy harvesters). When the sensor node is not performing sensing, computing, or processing operations, it is forced into sleep mode, where it consumes negligible amounts of energy. Fig. 2 shows a snapshot of the power profile of an IoT node consisting of two modes: sleep mode (when it is neither performing sensing, computing, or communication functions) and active mode (when it wakes up to perform sensing, computing, or communication operations). From the power profile, the average power consumption of the node is

$$P_{node} = D \cdot P_{act} + (1 - D) \cdot P_{sleep} \tag{1}$$

where,

$$D = \frac{t_{act}}{t_{act} + t_{sleep}} \tag{2}$$

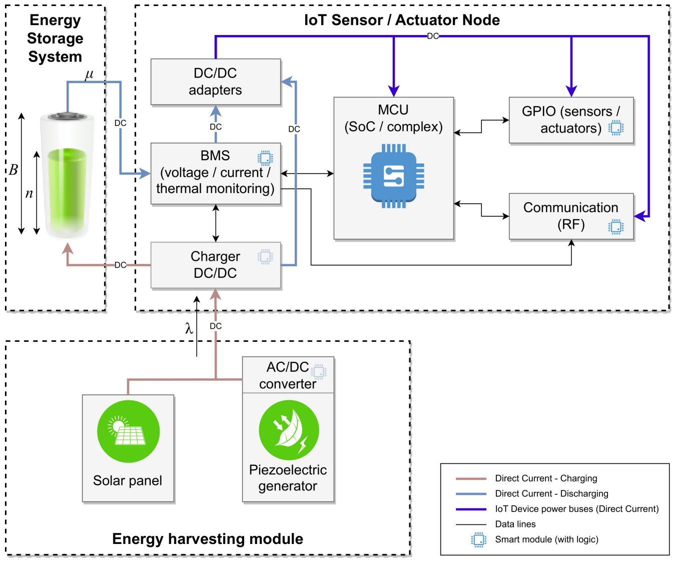

Figure 1. The architecture of a self-powered Green IoT sensor node

t_{act} is the time spent in the active mode and t_{sleep} is the time spent in the sleep mode. P_{act} is the power consumption of the node in the active mode, and P_{sleep} is the power consumption of the node in the sleep mode. The energy consumed during the active mode is the sum of the energy consumed by the sensing, computing, communication units and other auxiliary electronics components of the node during the active period.

The power profile in Fig. 2 is presented to illustrate the characteristics of the IoT energy consumption model, which forms the basis of our energy packetisation or quantisation model in the following subsection. The power profile is obtained using a laboratory testbed that consists of two IoT nodes positioned 2 m apart along a high-pressure plastic pipe measuring 12 m in length and with a diameter of 25 mm. In order to optimise or minimise the energy consumption of the IoT nodes, the nodes are configured to perform distributed computing with Kalman filtering (by sharing the computing load), adaptive sensing (by using an energy-efficient but less accurate accelerometer sensor and an energy-hungry but more accurate accelerometer sensor), and duty cycling (forcing the node to enter sleep modes when it is idle).

Performing energy planning of self-powered IoT nodes requires an estimate of the energy demand, energy generation, and storage capacity to ensure a low probability of service outage and a long lifetime for the node. From the characterisation of the energy harvesting system (e.g., solar cells, piezoelectric, RF, or thermoelectric energy harvester), the power profile can be obtained. An empirical power profile of a solar energy harvester for an IoT node is shown in Kuzman et al. (2019), which consists of active periods of solar power generation (when there is enough solar radiation) and a period of no solar power generation (when there is insufficient solar radiation notably during the night). From the energy consumption and generation profile, the mean energy produced and consumed can be estimated. The mean energy generated and consumed can be used to determine the number of energy packets produced and consumed per unit of time, as discussed in the next section.

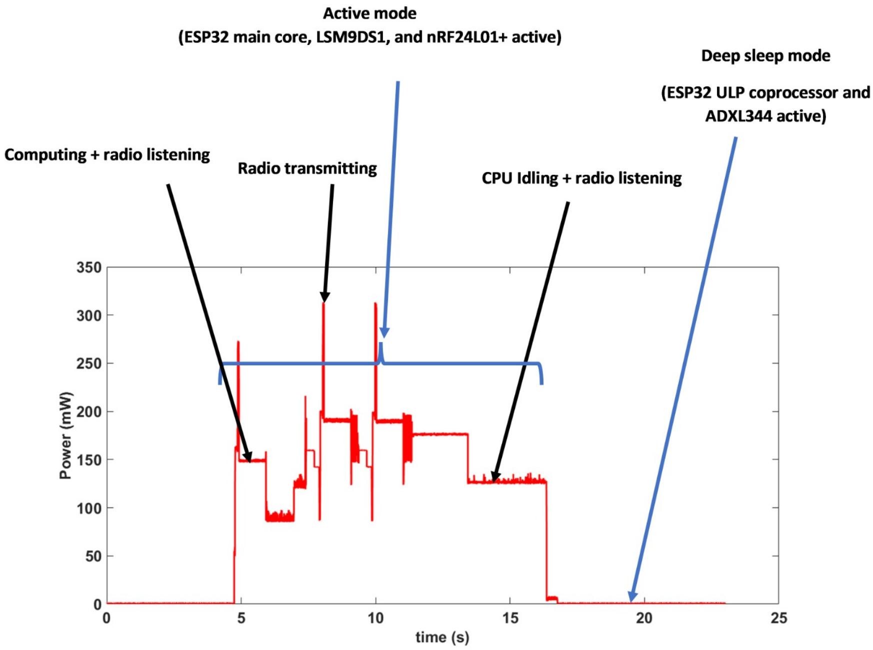

Figure 2. A snapshot of the power profile of an IoT node

2.2 The energy packet model of the node

In order to discretise or quantise energy into energy packets, the first step is to determine the quantisation step, which, in our case, is the size of the energy packet. We consider an energy packet (in mWh or mAh) as a pulse of power or current which lasts for a defined time duration. Assuming that energy is consumed during active periods when the node wakes up to perform sensing, computing, or communication (and that a negligible amount of energy is consumed during the deep sleep period), the size of the energy packet can be considered to be $E_p = P_{act} \cdot t_{act}$. However, the quantisation step can be set to any arbitrary value but must be kept consistent in the quantisation of the energy harvesting, consumption, and storage processes as in Da Silva et al. (2017).

Let C_B (measured in mWh) represent the capacity of the energy storage system (ESS) which may be battery or a supercapacitor, and then the capacity of the ESS (in energy packets) is $B = C_B/E_p$. That is, the number of energy packets that can be stored in the ESS is B, and the energy states of the ESS are $\{0, 1, 2, \cdots, B\}$. We assume that the node wakes up only when triggered by a random event (e.g., leakage of fluids from a pipe in the case of a pipeline monitoring system). In this case, the energy drawn from the battery per time unit is scattered independently and uniformly in the sense of a Poison process Kaj and Konané (2016). The energy consumption process becomes $E_{node} = t_{act} \cdot P_{act} N_t^{(1/t_i)}$, where N_t^{μ} denotes a standard Poisson process on the half line with constant intensity μ. That is, energy is drawn from the battery in small jumps of energy $E_p = t_{act} \cdot P_{act}$ which occur interspaced by independent and exponentially distributed waiting times with expected value $t_i = t_{act} + t_{sleep}$. From the power consumption profile, the mean number of energy packets drawn from the energy storage system per time unit in the time interval $[0,\ t_i]$ is

$$\mu = \frac{t_{act}}{t_{act} + t_{sleep}} \cdot \frac{P_{act}}{E_p} \tag{3}$$

We consider an intermittent energy harvesting source (e.g., the presence of solar radiation, light, vibration, wind, RF radiation, and heat). For simplicity, we assume that the energy arrival times of the energy packets follow a Poisson process with rate λ_H Ng et al. (2013); Wang et al. (2014). This assumption may be realistic in self-powered IoT nodes that stay in a deep sleep mode for a time that is exponentially distributed. They wake up to receive or transmit data packets, harvest wireless RF energy at the same time and then return to sleep mode. From the power generation profile of the energy harvester, the number of energy packets generated per time unit in the time interval $[0,\ T]$ is

$$\lambda_H = \frac{1}{E_p \cdot T} \int_0^T P_H(\tau)\, d\tau. \tag{4}$$

where $P_H(t)$ is the output energy profile of the energy harvesting system. If the harvested energy is greater than the energy required to power the IoT node, the surplus is stored in the battery to be used when the node's needs are greater than the energy production. From the energy conservation principle and assuming that there is no energy leakage from the ESS, the mean number of energy packets delivered to the battery is $\lambda = \mu - \lambda_H$, which also follows a Poisson process. In this case, the process of delivering energy packets of the battery is also assumed to follow a Poisson process with mean rate $\lambda = \lambda_H - \mu$.

2.3 Markov model of energy storage system with multiple energy thresholds

Suppose that the storage space of the energy storage system (ESS) is partitioned into m non-overlapping intervals called energy-saving regimes by introducing $m-1$ energy-saving thresholds (or barriers, or switches). In the m^{th} interval (with the highest energy content), the IoT node is fully functional and performs all its functions typically. However, in the subsequent intervals, some of the functionalities of the node may be limited or disabled to save energy to prolong the lifetime of the device, making the node semi-functional. In the first interval (with the lowest energy content), most of the functionalities (computation and communication) of the nodes are significantly limited or disabled; that is, the node is non-functional. Therefore, the node's mean rate of energy consumption depends on the energy content of the energy storage system and is given by

$$\mu(n) = \begin{cases} \mu_1 & 0 < n \leq K_1\ , \\ \mu_2 & K_1 < n \leq K_2\ , \\ \mu_3 & K_2 < n \leq K_3\ , \\ \cdots & \cdots\ , \\ \mu_m & K_m < n \leq B. \end{cases} \tag{5}$$

By introducing energy thresholds and reducing energy consumption at the node as the energy content of the ESS goes below the various thresholds, the lifetime of the node can be increased. For certain IoT sensors, the energy consumption can be reduced on the fly by throttling the speed of the processor clock, decreasing the operating voltage, or decreasing the transmission power. The drawback of forcing the node to enter into energy saving modes is that it may degrade the quality of service of the nodes and should only be considered only when the energy stored in the ESS is below certain critical thresholds and sacrificing some level of performance is acceptable. Energy modes for some IoT devices may include: run mode (CPU, flash, SRAM, and peripheral on), doz mode (CPU clock runs slower than peripheral on), idle mode (CPU off, flash, SRAM, and peripheral on), sleep mode (CPU, flash, SRAM off, and peripheral on), and deep sleep mode (CPU, flash, SRAM, and peripheral off), Evanchuk (2024).

In the ESS model, we assume that energy is delivered and consumed by quantoms (energy packets). The process resembles the behaviour of a queueing system. The energy packets are like customers and the time to consume one packet corresponds to service time. The number of customers on the queueing system denotes the energy in ESS. This allows us to make use of the existing queueing models.

We model the dynamic changes in the number of energy packets in the energy storage system (ESS) as an M/M(n)/1/B queueing Markov process $\{N(t)|t \geq 0\}$, such that $p(n,t) = \Pr\{N(t) = n\}$ is the probability of having n energy packets in the ESS. In the notation, based on Kendall (1953), it is a station with Poisson input, exponantially distributed service time, single server and limited to B number of customers inside. M(n) underlines that the parameter μ of the time to consume an energy packet may depend on the queue length (number of energy packets in the ESS), $\mu = \mu(n)$. The model consists of a set of equations, see, e.g. Kleinrock (1975):

$$\begin{aligned}
\frac{dp(0,t)}{dt} &= -\lambda p(0,t) + \mu(1)p(1,t), \\
\frac{dp(n,t)}{dt} &= -(\lambda + \mu_1)p(n,t) + \lambda p(n-1,t) + \mu(n)p(n+1,t), \qquad n = 1, \dots B-1, \\
\frac{dp(B,t)}{dt} &= \lambda p(B-1,t) - \mu(B)p(B,t).
\end{aligned} \tag{6}$$

This sytem has well known solution, both in transien and steady states if the parameter μ does not depend on n, but in caase of $\mu(n)$ the soltion is limited to steady state when state probabilities do not depend on time. Therefore in Section 3.2 we analyse its transient state in detail.

The model can be extended to the case where the distributions between the time of arrival of energy packets and the distributions of the time of their consumption are not exponential but are a linear combination of exponentially distributed phases that can approximate any distribution. Many software tools adapt the parameters of such distributions to the actual measurement data, e.g. Asmussen et al. (1990), Bause et al. (2010), as well as tools to solve numerically the resulting Markov chain equations, e.g. Prism, Kwiatkowska et al. (2011) or our Olymp, Pecka et al. (2018).

3 THE ENERGY PERFORMANCE ANALYSIS

The equations in (6) above are solved to determine the performance metrics such as the mean number of energy packets in the ESS, the probability that all the energy packets stored in the ESS are depleted, the probability that ESS is full and energy packets that arrive after the ESS is full are lost (energy wastage probability), and the density of the lifetime of the node. We perform both the steady state and transient state analysis of the performance of the ESS to provide more insights into the influence of the mean number of energy packets delivered to the ESS, the mean energy consumption rate, and the energy threshold(s) on the energy performance of the node.

3.1 Steady-state analysis

In steady-state, when $\lim_{x\to\infty} p(n,t;n_0) = p(n)$, the differential equations above become linear equations which can be easily solved to derive the steady-state distribution of the number of energy packets in the ESS and the probability $p(0)$ of depleting all the energy packets stored in the ESS (probability that the ESS is empty). The steady-state distribution of the number of energy packets in the ESS is, e.g. Kleinrock (1975)

$$p(n) \quad = \quad p(0)\,\frac{\lambda^n}{\mu(1)\ \cdots\ \mu(n)}\,, \tag{7}$$

and taking normalization $\sum_{n=0}^{B} p(n) = 1$, the probability $p(0)$ of depleting all the energy packets stored in the ESS is

$$p(0) = \frac{1}{1+\sum_{n=1}^{B}\{\lambda^n/\prod_{i=0}^{n-1}\mu(i+1)\}}\,.$$

From the equation above, the steady-state probability $p(B)$ that the ESS is full can be derived. The energy storage space of the energy storage systems (e.g., battery or supercapacitor) for IoT nodes is very limited (especially for very small and mobile IoT nodes), and energy packets that arrive when the ESS is full are lost, resulting in undesirable energy wastage. Also, when all the energy packets stored in the ESS are depleted, the node shuts down, interrupting the service provided by the node. Thus, the probability $p(0)$ is a critical performance metric and can be considered the service outage probability. In the case of a single threshold, K, there are two energy consumption regimes with $\mu(u) = \mu_1$ (for $n < K$) and $\mu(n) = \mu_2$ (for $n > K$) and the performance metrics are also a function of the energy threshold K.

3.2 Transient-state analysis

We present the transient-state analysis of the energy performance of the ESS with energy thresholds. The steady-state analysis assumes that the mean rate at which energy packets are delivered to the ESS and the mean rate at which energy packets are consumed from the ESS are constant. However, the mean number of energy packets harvested may vary within 24 24-hour day period and between various days and months. In the case of solar energy harvesters, sufficient energy is generated during the solar hour period of the day, and no energy is generated at night. There are also fluctuations within the day that may result in fluctuations in the mean number of energy packets harvested and the mean number of energy packets delivered to the ESS. These time-dependent changes in the number of energy packets harvested and delivered to the ESS make transient analysis of the dynamic changes in the energy content of the ESS interesting. In the transient-state analysis, the performance metrics considered in the previous section on steady-state analysis become time-dependent.

Transient anlysis of M/M/1/B was performed in Tákacs (1962), Morse (1958), Sharma and Gupta (1982), and recently in Massey et al. (2023). Here, we extend it to the case of M/M/(n)/1/B, i.e. state-dependent parameters $\mu(n)$. The most straightforward approach is to consider the Eqs. (6) in Laplace domain

$$\begin{aligned} sP(0,s) - p(0,0) &= 1 - \lambda P(0,s) + \mu_1 P(1,s) \\ sP(n,s) - p(n,0) &= -[\lambda + \mu(n)]P(n,s) + \lambda P(n-1,s) + \mu_1 P(n+1,s) \quad 1 \le n < B \\ sP(B,s) - p(B,0) &= \lambda P(B-1,s) - \mu_B P(B,s) \quad n = B. \end{aligned} \tag{8}$$

where

$$P(n,s) = \mathscr{L}p(n,t) = \int_0^{\infty} e^{-st} p(n,t)dt \ \text{ and } \ \mathscr{L}\{\frac{p(n,t)}{dt}\} = sP(n,s) - p(n,0),$$

solve the system (8) for the values of s needed by the inversion algorithm and then look numerically for the originals of $P(n,s)$, e.g. with the use of Stehfest algorithm Stehfest (1970):

$$p(n,t) = \frac{\ln 2}{t} \sum_{i=1}^{N} V_i \, P(n, s = \frac{\ln 2}{t} i) \, ,$$

and

$$V_i = (-1)^{N/2+i} \sum_{k=\lfloor \frac{i+1}{2} \rfloor}^{\min(i,N/2)} \frac{k^{N/2+1}(2k)!}{(N/2-k)!k!(k-1)!(i-k)!(2k-i)!} \, ,$$

in our numerical computations, we used $N = 20$.

However, we present also the explicit expressions for $P(n,s)$. Below, we do it for the case when the buffer is initially empty, $p(0,0) = 1$. Similarly, results can be obtained for a 'mirror' process that starts at B and ends at 0.

Assume that $\mu(n)$ takes m values specific for m zones, as defined in Eqs. (5). Starting from the equations in the first interval (e.g., $1 \le n \le K_1 - 1$),

$$\lambda \frac{P(n-1,s)}{P(n,s)} = \left[(s+\lambda+\mu_1) - \mu_1 \frac{P(n+1,s)}{P(n,s)} \right] \tag{9}$$

Dviding both sides of Eq. (9) by μ_1, we get

$$\frac{\lambda}{\mu_1} \frac{P(n-1,s)}{P(n,s)} = \left[(\frac{s}{\mu_1} + \frac{\lambda}{\mu_1} + 1) - \frac{P(n+1,s)}{P(n,s)} \right] . \tag{10}$$

From Eq. (9),

$$\frac{P(n+1,s)}{P(n,s)} = \frac{\lambda}{\left[(s+\lambda+\mu_1) - \mu_1 \frac{P(n+2,s)}{P(n+1,s)} \right]} \tag{11}$$

and substituting (11) in (10) we get

$$\frac{\lambda}{\mu_1} \frac{P(n-1,s)}{P(n,s)} = \left[(\frac{s}{\mu_1} + \frac{\lambda}{\mu_1} + 1) - \frac{\lambda}{\left[(s+\lambda+\mu_1) - \mu_1 \frac{P(n+2,s)}{P(n+1,s)} \right]} \right] \tag{12}$$

which can be rearranged as

$$\frac{\lambda}{\mu_1} \frac{P(n-1,s)}{P(n,s)} = \left[(\frac{s}{\mu_1} + \frac{\lambda}{\mu_1} + 1) - \frac{\frac{\lambda}{\mu_1}}{\left[(\frac{s}{\mu_1} + \frac{\lambda}{\mu_1} + 1) - \frac{P(n+2,s)}{P(n+1,s)} \right]} \right] . \tag{13}$$

The ratio $\frac{\lambda}{\mu_1}\frac{P(n-1,s)}{P(n,s)}$ can be expressed as a Hyper Geometric series as follows:

$$\frac{\lambda}{\mu_1}\frac{P(n-1,s)}{P(n,s)} = \left[\left(\frac{s}{\mu_1}+\frac{\lambda}{\mu_1}+1\right) - \frac{\frac{\lambda}{\mu_1}}{\left[\left(\frac{s}{\mu_1}+\frac{\lambda}{\mu_1}+1\right) - \frac{\frac{\lambda}{\mu_1}}{\left(\frac{s}{\mu_1}+\frac{\lambda}{\mu_1}+1\right)-\cdots}\right]}\right] \tag{14}$$

We apply the concepts of Hyper Geometric Functions, Lorentzen and Waadeland (1992) and Finite Continued Fractions Waadeland and Lorentzen (2008); Ikenaga (2022, accessed on 12 February, 2022) to simplify the Hyper Geometric series in Eq. (14). Let

$$x = \left[\left(\frac{s}{\mu_1}+\frac{\lambda}{\mu_1}+1\right) - \frac{\frac{\lambda}{\mu_1}}{\left[\left(\frac{s}{\mu_1}+\frac{\lambda}{\mu_1}+1\right) - \frac{\frac{\lambda}{\mu_1}}{\left(\frac{s}{\mu_1}+\frac{\lambda}{\mu_1}+1\right)-\cdots}\right]}\right],$$

which can also be expressed as

$$x = (a+b) - \frac{b}{(a+b) - \frac{b}{(a+b)-\frac{b}{(a+b)-\cdots}}},$$

where $a = \frac{s}{\mu_1}+1$ and $b = \frac{\lambda}{\mu_1}$. Since x contains a copy of itself as the bottom of the first fraction, it can be expressed as

$$x = (a+b) - \frac{b}{x} \tag{15}$$

The roots of Eq. (15) are

$$x = \frac{(a+b)\pm\sqrt{(a+b)^2-4b}}{2}. \tag{16}$$

Since the fraction is positive, we take the positive root

$$x = \frac{(a+b)+\sqrt{(a+b)^2-4b}}{2}. \tag{17}$$

From Eq. (14)

$$P(n,s) = \frac{2b}{(a+b)+\sqrt{(a+b)^2-4b}}P(n-1,s) \tag{18}$$

Therefore, for $1 \le n < K_1$, the transient state probabilities $P(n,s)$ are given by

$$P(n,s) = \left(\frac{\lambda}{\mu_1}\frac{1}{x}\right)^n \tag{19}$$

where

$$x = \frac{s+\lambda+\mu_1+\sqrt{(s+\lambda+\mu_1)^2-4\lambda\mu_1}}{2\mu_1}$$

Applying the above solution iteratively for all intervals, we obtain the transient state probabilities as follows:

$$P(n,s)=\begin{cases}\left(\dfrac{\lambda}{\mu_1}\dfrac{1}{\alpha_1(s)}\right)^n P(0,s), & 1\le n\le K_1\ ,\\ \left(\dfrac{\lambda}{\mu_2}\dfrac{1}{\alpha_2(s)}\right)^n P(0,s), & K_1< n\le K_2\ ,\\ \left(\dfrac{\lambda}{\mu_3}\dfrac{1}{\alpha_3(s)}\right)^n P(0,s), & K_2< n\le K_3\ ,\\ \cdots & \cdots\ ,\\ \left(\dfrac{\lambda}{\mu_{m-1}}\dfrac{1}{\alpha_{m-1}(s)}\right)^n P(0,s), & K_{m-2}< n\le K_{m-1}\ ,\\ \left(\dfrac{\lambda}{\mu_m}\dfrac{1}{\alpha_m(s)}\right)^n P(0,s), & K_{m-1}< n\le B-1.\end{cases} \tag{20}$$

where

$$\alpha_i(s)=\frac{s+\lambda+\mu_i+\sqrt{(s+\lambda+\mu_i)^2-4\lambda\mu_i}}{2\mu_i},\quad i=1,2,3,\cdots m.$$

From the first equation in (8),

$$(s+\lambda)P(0,s)=1+\mu_1P(1,s)$$

we obtain $P(0,s)$

$$P(0,s)=\frac{(a+b)+\sqrt{(a+b)^2-4b}}{(s+\lambda)[(a+b)+\sqrt{(a+b)^2-4b}]-2\lambda} \tag{21}$$

which can be rearranged to obtain

$$P(0,s)=\frac{s+\lambda+\mu_1+\sqrt{(s+\lambda+\mu_1)^2-4\lambda\mu_1}}{(s+\lambda)\{s+\lambda+\mu_1+\sqrt{(s+\lambda+\mu_1)^2-4\lambda\mu_1}\}-2\lambda\mu_1}. \tag{22}$$

From the last equation of (8),

$$(s+\mu_m)P(B,s)=\lambda P(B-1,s)$$

and $P(B,S)$ can be expressed as follows:

$$P(B,s)=\frac{\lambda}{s+\mu_m}\left(\frac{\lambda}{\mu_m}\frac{1}{\alpha_m(s)}\right)^{B-1}P(0,s). \tag{23}$$

We remind that in the case of an M/M/1/B model, the transient solutions obtained in Sharma and Gupta (1982), for the same initial condition $p(0,0)=1$ and $p(n,0)=0$, $n=1,\dots B$ is

$$P(n,s)=\frac{(\alpha\beta)^n[\alpha^{B-n+1}-\beta^{B-n+1}]-(\alpha\beta)^{n+1}[\alpha^{B-n}-\beta^{B-n}]}{s[\alpha^{B+1}-\beta^{B+1}]} \tag{24}$$

where

$$\alpha(s)=\frac{s+\lambda+\mu+\sqrt{(s+\lambda+\mu)^2-4\lambda\mu}}{2\mu},$$

and

$$\beta(s) = \frac{s + \lambda + \mu - \sqrt{(s + \lambda + \mu)^2 - 4\lambda\mu}}{2\mu}.$$

Similarly,

$$P(0,s) = \frac{[\alpha^{B+1} - \beta^{B+1}] - (\alpha\beta)[\alpha^B - \beta^B]}{s[\alpha^{B+1} - \beta^{B+1}]} \tag{25}$$

and

$$P(B,s) = \frac{(\alpha\beta)^B[\alpha - \beta]}{s[\alpha^{B+1} - \beta^{B+1}]}. \tag{26}$$

For very large values of B, the transient solution reduces to an M/M/1 model as follows

$$\lim_{B\to\infty} P(n,s) = \frac{(1-\beta)\varrho^n}{s\alpha^n} \tag{27}$$

where $\varrho = \lambda/\mu$ is the energy supply to demand ratio.

For other initial conditions, the system of eqautions in (8) is solved numerically. The mean number of energy packets in the ESS at time t is

$$E[N(t)] = \sum_{n=0}^{B} np(n.t) \tag{28}$$

The Laplace transforms above can be inverted numerically using the Stehfest algorithm to obtain $p(n,t)$ from which time-dependent performance metrics such as the service outage probability $p(0,t)$, energy wastage probability $p(B,t)$, and the mean number of energy packets in the ESS $E[N(t)]$ can be obtained.

3.3 Modelling the lifetime of the IoT node

We investigate the impact of the threshold energy management policy on the device's lifetime. The objective of introducing the adaptive threshold (or imposing the energy-saving regimes) is to increase the device's lifetime. The device's lifetime is the time required to deplete all the energy packets stored in the ESS Kuaban et al. (2023b); Czachórski et al. (2022). We model the device's lifetime as the first passage time of the M/M(n)/1/B model from any starting state to $n = 0$. The density of the first passage time, $\gamma_{i,0}(t)$ of the process that start at $n = i$ and is absorbed at $n = 0$ can be obtained numerically by solving the proposed M/M(n)/1/B model.

We compute the first passage time from B to zero of the proposed M/M/(n)/1/B model by making state zero the absorbing one, i.e. modifying the first equation of the system ((6) to the form

$$\frac{dp(0,t)}{dt} = \mu(1)p(1,t);$$

if the $p(1,t)$ is computed for the chain initiated from state B, the intensity of entering state 0 in the equation above, is the density of the first passage time from B to 0,

$$\gamma_{B,0}(t) = \mu(1)p(1,t); \tag{29}$$

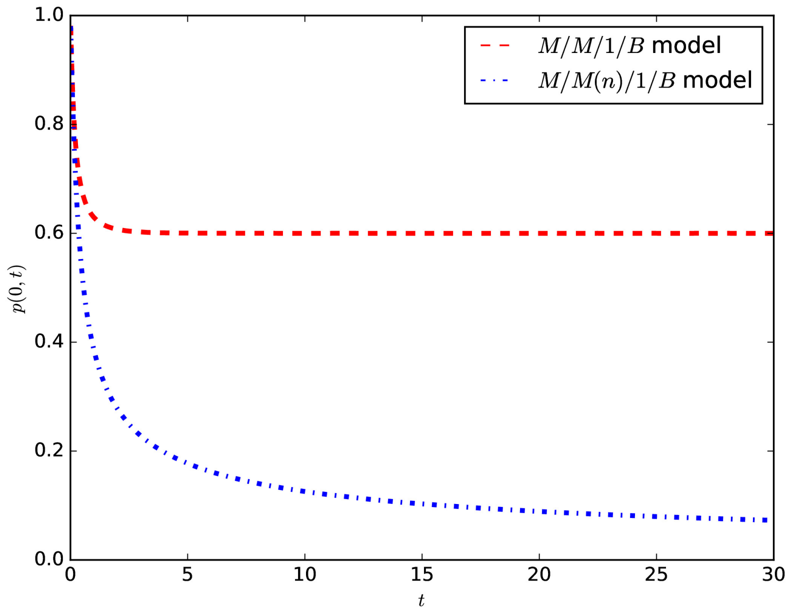

Figure 3. Comparing the transient probability of service outage, $p(0, t)$ from the M/M/1/B and M/M(n)/1/B for $\mu_1 = 2$, $\mu_2 = 5$, $\lambda = 2$, $K = 40$, and $B = 100$.

Similarly, to model the first passage time from 0 to B (the time required to charge the ESS to its full capacity), we make B the absorbing state and compute $p(B-1, t)\lambda$ in chain initiated at state 0.

$$\gamma_{0,B}(t) = \lambda p(B-1, t). \tag{30}$$

The performance metrics $\gamma_{B,0}$ (lifetime of the node) and $\gamma_{0,B}$ can be obtained numerically using a Markov solver developed in Pecka et al. (2018).

4 NUMERICAL RESULTS

In the numerical results presented, we consider a battery with a charge rating $Q = 2100$ mAh, debth of discharge, $DoD = 70\%$, and voltage $v = 3.7$ volts. The energy capacity of the battery, $C_B = 2100 * 0.7 * 3.7 = 5439$ mWh. We assume that the quantisation step (size of an energy packet) is $E_p = 54.39$ mWh and the capacity of the battery in energy packets (maximum number of packets that can be stored in the battery) is $B = 5439/54.39 = 100$ energy packets. Assuming that the mean energy delivered to the battery is 108.78 mWh, then the mean number of packets delivered to the battery per hour is $\lambda = 108.78/54.39 = 2$ energy packets per hour. Similarly, the mean number of energy packets consumed per hour is obtained. For each numerical example, we provide the values of the various parameters under the figure.

4.1 Energy performance of an IoT node with a non-solar renewable energy source

The steady-state and transient-state analyses presented in section 3 above are more applicable to non-solar energy sources. That is, energy sources that can produce energy both in the day and in the night (e.g., RF, vibration, wind, etc.). Figs. 4 - 7 present the results obtained using the analytical model models presented in the previous section.

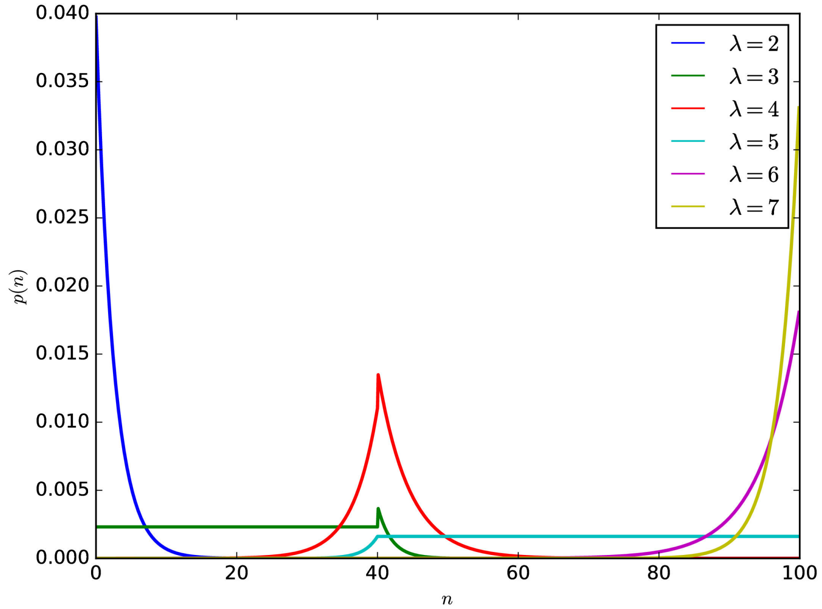

Figure 4. The influence of λ on the probability of having n energy packets in the battery, for $\mu_1 = 3$, $\mu_2 = 5$, $B = 100$, $K = 40$

Figs. 3, present the changes of the service outage probability, $p(0,t)$ as a function of time until attaining a steady state. The results compares two cases; one with threshold and the other without a threshold. The introduction of a threshold significantly reduces the probability of service outage, $p(0,t)$.

Fig.4 illustrates the above solution in the case where the battery volume is $B = 100$ energy units. The only threshold is placed at $K = 40$, the consumption rates are $\mu(n) = \mu_1 = 3$ energy units per time unit, $n = 1, \ldots K$; $\mu(n) = \mu_2 = 5$ energy units per time unit, $n = 41 \ldots B$. Depending on the value of harvesting rate λ, the probability mass of $p(n)$ is concentrating close to 0 ($\lambda < \mu_1$), close to B ($\lambda > \mu_2$) or around K ($\mu_1 < \lambda < \mu_2$). If $\lambda = \mu_1$. The distribution does not change in the corresponding interval or $\lambda = \mu_2$.

Fig.5 presents the impact of λ, K, and μ_1 on the probability $p(0)$ of empty battery, when $\mu_2 = 5$, $B = 100$, $K = 40$. Obviously, increasing the intensity of energy delivery and reducing energy consumption in the economical mode reduce the likelihood of energy depletion.

Figs. 6, 7 display the density of the lifetime of the IoT node $\gamma_{B,0}(t)$ for various values of the threshold $K = 20, 40, 60$ and various values of $\mu_1 = 2.5, 3, 4$; $\mu_2 = 5$ is not changing. The densities are compared with the same density when there is no threshold, and the unique rate is $\mu = 5$. The impact of the energy saving – of the threshold K and reduced consumption rate μ_1 is important. It influences not only the mean time to depletion but also the variance of the distribution.

4.2 Energy performance of an IoT node with a Solar energy source

The energy produced by non-solar energy sources (e.g., RF, vibration, wind, etc.) is relatively small and may be insufficient for some energy-hungry IoT nodes. A scalable approach to generate sufficient energy to power an IoT node is the use of solar energy. However, solar energy sources produce energy during the day and do not produce energy during the night, but energy may be consumed during the night. Thus,

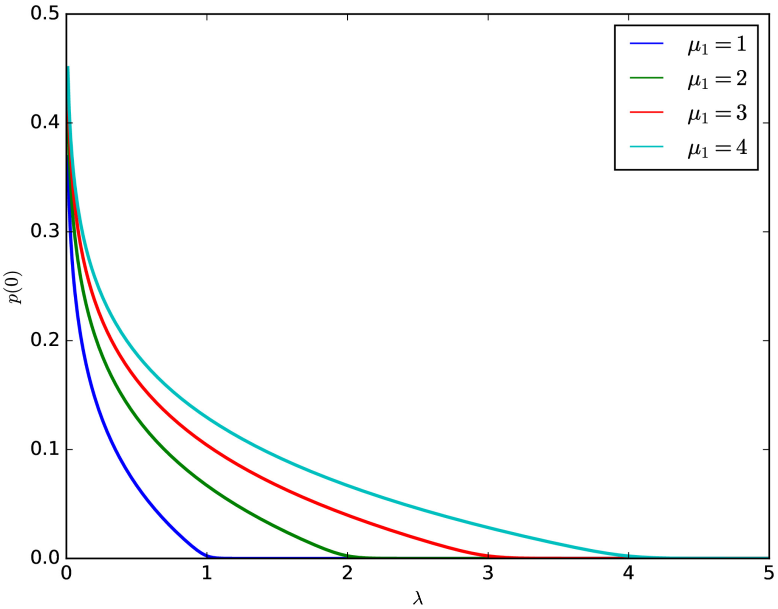

Figure 5. The influence of μ_1 on the probability of empty battery, $p(0)$ for $\mu_2 = 5$, $B = 100$, $K = 40$

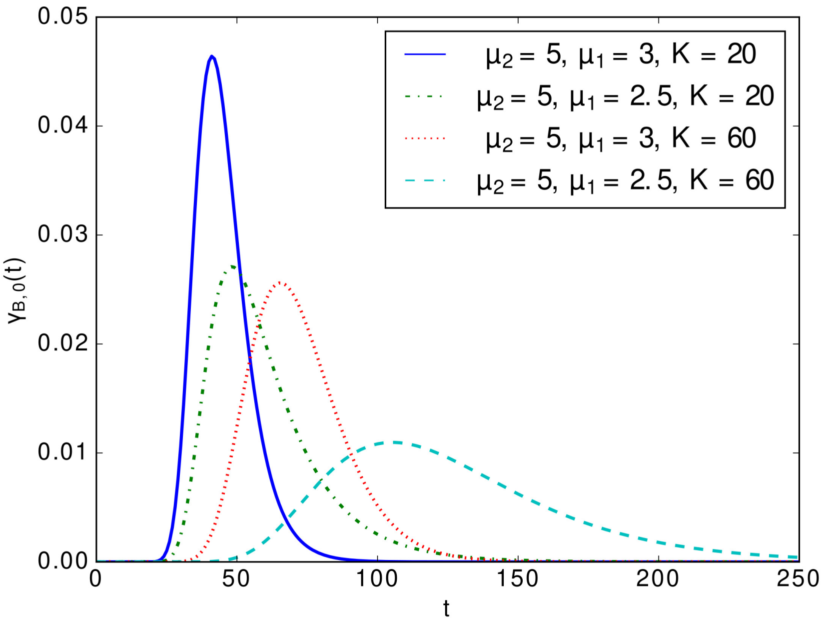

Figure 6. The influence of the proposed energy-saving threshold policy on the density of the lifetime of the IoT node $\gamma_{B,0}(t)$, for $K = 20, 60$, $\mu_2 = 5$, $\lambda = 2$, $B = 100$.

the analysis presented in section 3 is not sufficient to analyse energy storage systems that are supplied by energy from solar energy sources.

In this case, the performance metrics are obtained by solving the differential equation equation in (6) numerically considering various initial conditions, $N(0) = n_0$, mean charging rate, λ, mean energy

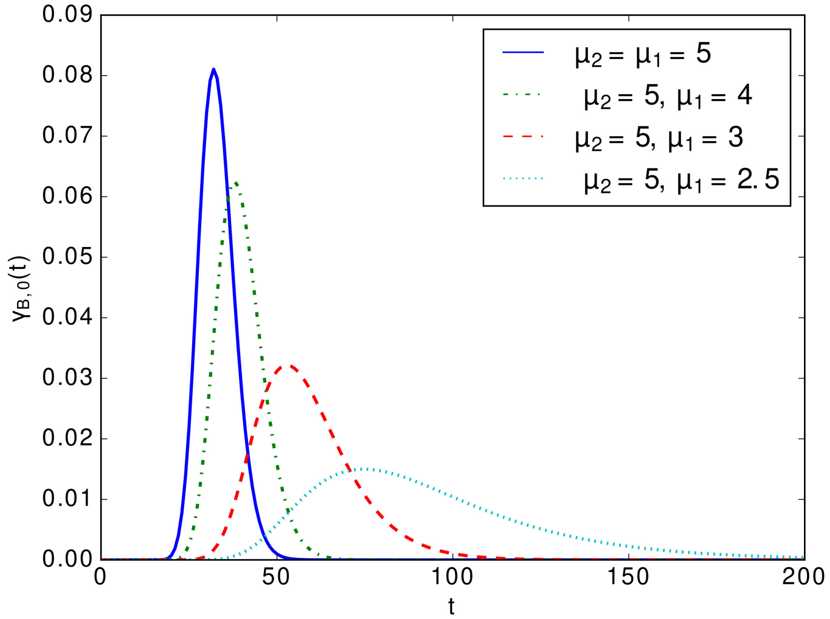

Figure 7. The influence of μ_1 on the density of the lifetime of the IoT node $\gamma_{B,0}(t)$, for $\mu_2 = 5$, $\lambda = 2$, $B = 100$, $K = 40$.

consumption rates, $\mu(n)$ (e.g., $\mu(n) = \mu_1$ for $n \leq K$ and $\mu(n) = \mu_2$ for $n \geq K$), and corresponding thresholds K. During the day, the ESS is charged with a mean rate of $\lambda - \mu(n)$ and during the night, $\lambda = 0$ and the ESS is discharged at a mean rate of $\mu(n)$. We can start with any initial condition (number of energy packets at $t = 0$). For example, we can start with $n_0 = B$ (B energy packets in the ESS) or $n_0 = 0$ (zero energy packets in the ESS). The distribution of the number of energy packets at the energy of the first day becomes the initial condition to obtain the distribution of the energy packet in the ESS during the night period (when the solar energy source is absent). Similarly, the distribution of the number of energy packets in the ESS at the end of the first night period becomes the initial condition for the evolution of the charging process for the second day. The process continues for several days as time evolves.

5 CONCLUSION

In this paper, we have investigated the practical implications of imposing energy-saving thresholds on the energy performance metrics of green IoT nodes. We conducted a steady-state and time-dependent analysis of the proposed energy packet-based model of the node, which considers the impact of switching the node to more energy-efficient regimes when the defined threshold of the energy content of the ESS is reached. We conducted numerical experiments to gain more insight into the extent to which the imposed energy threshold improves the energy performance of the green IoT node. We observed that configuring single or multiple thresholds improves the energy performance of the node significantly (e.g., increased lifetime of the node, reduced probability of service outage and energy wastage), and the value of the threshold(s) should be carefully chosen.

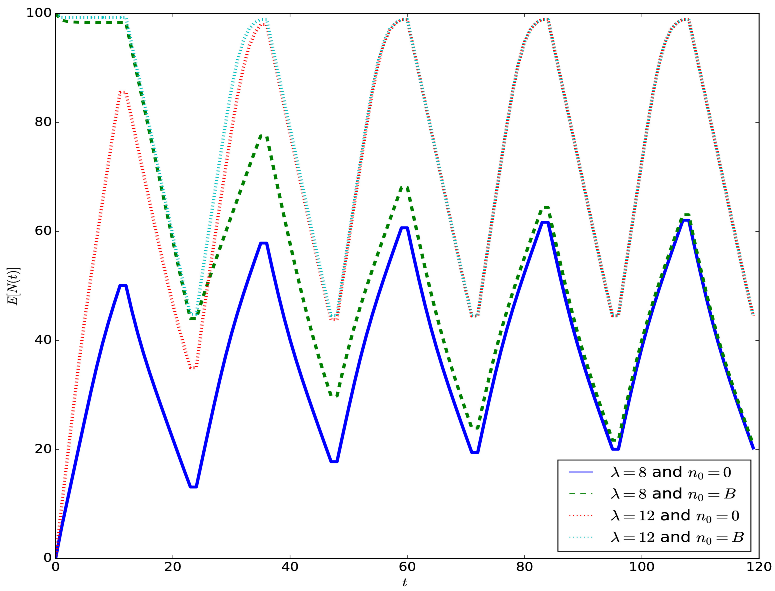

Figure 8. The dynamic evolution of the mean number of energy packets in the ESS, $E[N(t)]$: considering the cases with initial conditions $n_0 = 0$ (starting zero EPs in the ESS) and $n_0 = B$ (starting with B EPs in the ESS), $K = 40$.

CONFLICT OF INTEREST STATEMENT

There is are no financial, commercial or other relationships that might be perceived as a potential conflict of interest.

The authors declare that the research was conducted in the absence of any commercial or financial relationships that could be construed as a potential conflict of interest.

AUTHOR CONTRIBUTIONS

GSK: Writing-original draft, Conceptualization, Literature review, Modelling, Investigation, and numerical simulation. TC: Writing-original draft, Conceptualization, and supervision. EG: Writing-original draft, Conceptualization, and supervision. SS: Modelling and editing. PS: Modelling and editing. VN: Writing-original draft, Literature review, and editing. PP: Numerical simulation and Investigation. PC: Conceptualization, graphic design, and editing

FUNDING

This paper was partially supported by Reactive Too project that has received funding from the European Union's Horizon 2020 Research, Innovation and Staff Exchange Programme under the Marie Skłodowska-Curie Action (Grant Agreement No871163) and the international project co-financed by the program of the Minister of Science and Higher Education entitled "PMW" in the years 2021 - 2025; contract no. 5169/H2020/2020/2.

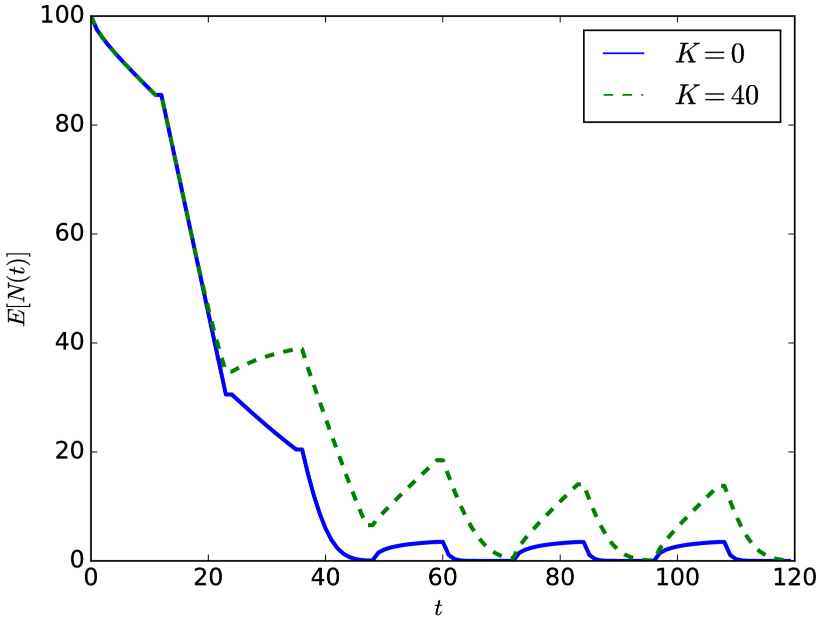

Figure 9. The dynamic evolution of the mean number of energy packets in the ESS, $E[N(t)]$: considering the case without threshold ($K = 0$) and the case with threshold ($K = 40$), $\lambda = 4$.

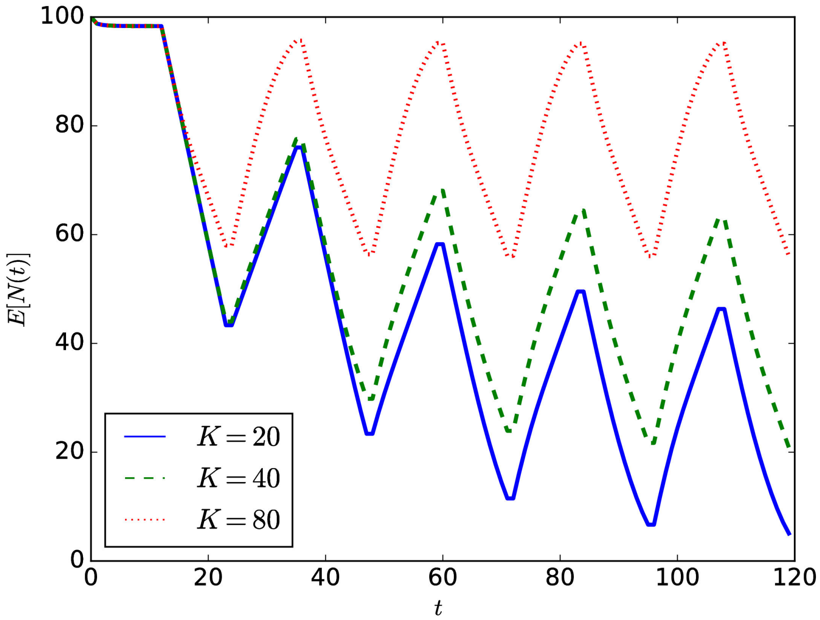

Figure 10. The influence of the energy threshold K on the dynamic evolution of the mean number of energy packets in the ESS, $E[N(t)]$, for $\lambda = 8$.

SUPPLEMENTAL DATA

None

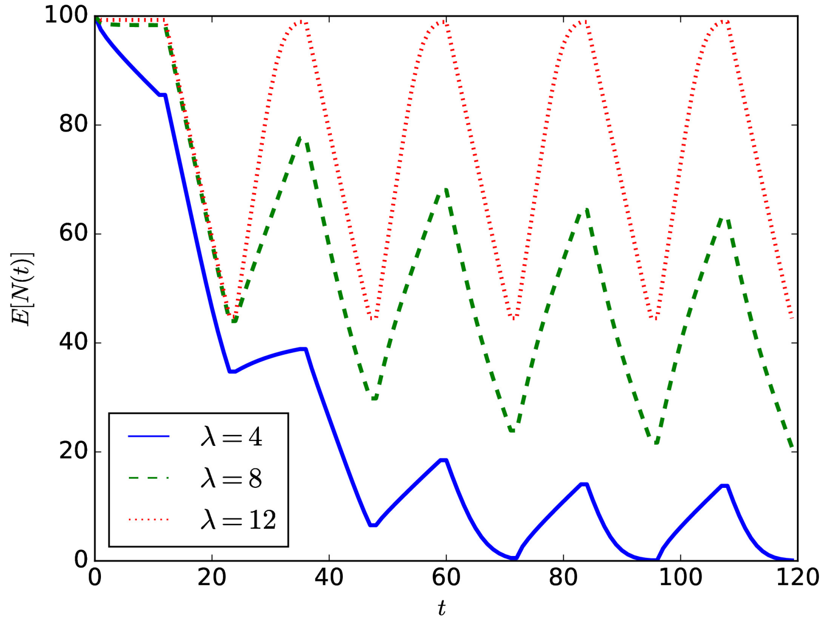

Figure 11. The influence of the mean charging rate λ on the dynamic evolution of the mean number of energy packets in the ESS, $E[N(t)]$, for $K = 40$.

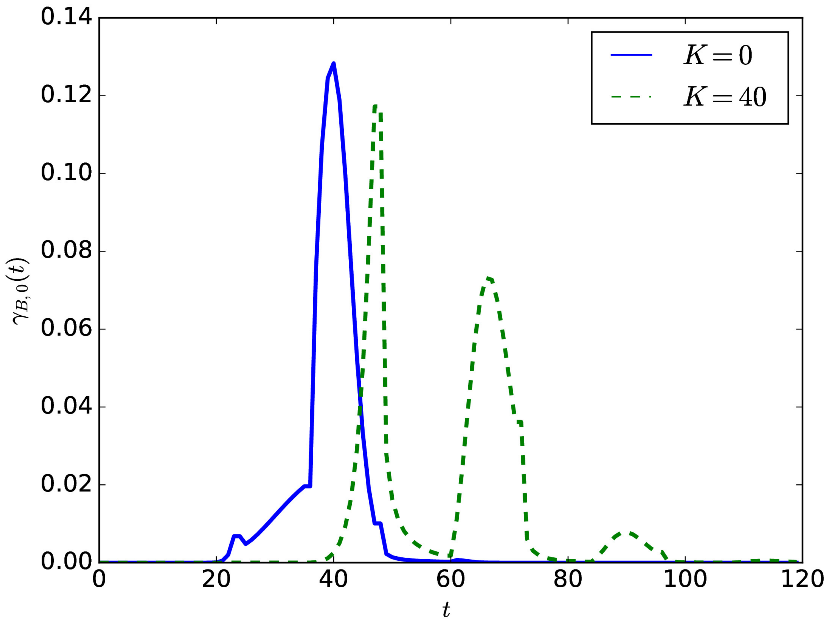

Figure 12. The density of the lifetime of the node, $\gamma_{B,0}(t)$: considering the case without threshold ($K = 0$) and the case with threshold ($K = 40$), $\lambda = 4$.

DATA AVAILABILITY STATEMENT

All the contribution and data are contained in the paper and any futher inquiries can be directed to the corresponding author of the paper.

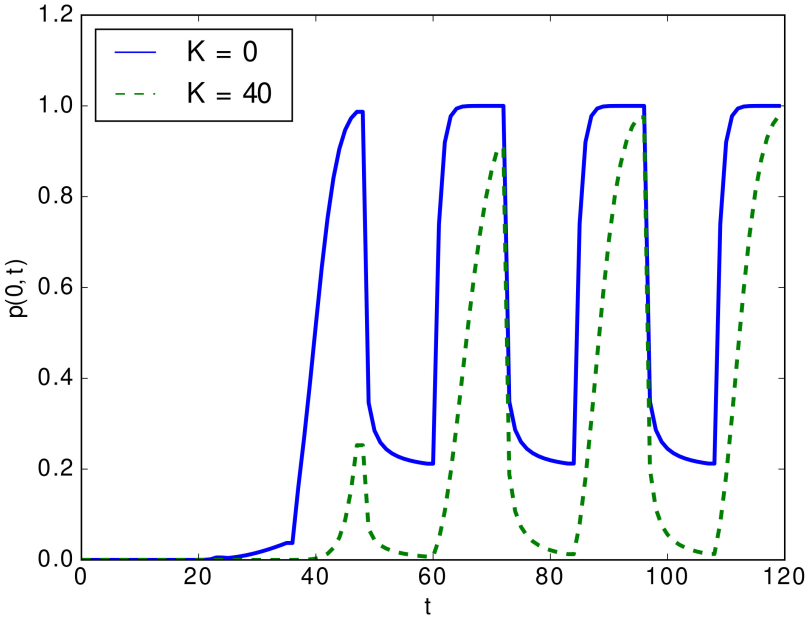

Figure 13. The dynamic evolution of the probability of service outage, $p(0,t)$: considering the case without threshold ($K = 0$) and the case with threshold ($K = 40$), $\lambda = 4$.

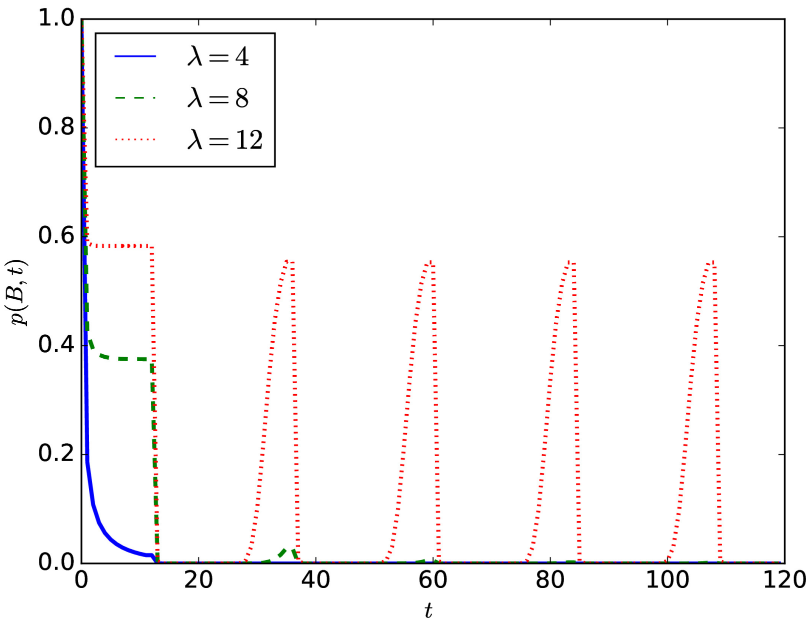

Figure 14. The influence of the mean charging rate λ on the probability of energy wastage, $p(B,t)$, for $K = 40$.

REFERENCES

377 Abdul-Qawy, A. S. H., Almurisi, N. M. S., and Tadisetty, S. (2020). Classification of energy saving
378 techniques for iot-based heterogeneous wireless nodes. *Procedia Computer Science* 171, 2590–2599

Al-Ansi, A., Al-Ansi, A. M., Muthanna, A., Elgendy, I. A., and Koucheryavy, A. (2021). Survey on intelligence edge computing in 6g: Characteristics, challenges, potential use cases, and market drivers. *Future Internet* 13

Albreem, M. A., Sheikh, A. M., Alsharif, M. H., Jusoh, M., and Yasin, M. N. M. (2021). Green internet of things (giot): applications, practices, awareness, and challenges. *IEEE Access* 9, 38833–38858

Alsharif, M. H., Jahid, A., Kelechi, A. H., and Kannadasan, R. (2023a). Green iot: A review and future research directions. *Symmetry* 15

Alsharif, M. H., Jahid, A., Kelechi, A. H., and Kannadasan, R. (2023b). Green iot: A review and future research directions. *Symmetry* 15, 757

Asmussen, S., Nerman, O., and Olsson, M. (1990). Fitting phase-type distributions via the em algorithm. *Scandinavian Journal of Statistics* 23, 419–441

Bause, F., Buchholz, P., and Kriege, J. (2010). Profido - the processes fitting toolkit dortmund, in proc. of the 7th international conference on quantitative evaluation of systems. *IEEE Computer Society* 96

Czachórski, T., Gelenbe, E., and Kuaban, G. S. (2022). Modelling energy changes in the energy harvesting battery of an iot device. In *Proceedings of the 2022 30th International Symposium on Modeling, Analysis, and Simulation of Computer and Telecommunication Systems (MASCOTS)* (Nice, France: IEEE), 81–88. doi:10.1109/MASCOTS56607.2022.00019

Da Silva, A. P. C., Renga, D., Meo, M., and Marsan, M. A. (2017). The impact of quantization on the design of solar power systems for cellular base stations. *IEEE Transactions on Green Communications and Networking* 2, 260–274

[Dataset] Evanchuk, E. (2024). Meeting power demand with energy harvesting in iot sensor nodes, https://www.digikey.pl/pl/articles/meeting-power-demand-with-energy-harvesting-in-iot-sensor-nodes, accessed on august, 2024

Gautam, A. and Dharmaraja, S. (2018). An analytical model driven by fluid queue for battery life time of a user equipment in LTE-A networks. *Physical Communication* 30, 213–219

Gelenbe, E. (2011). Energy packet networks: Ict based energy allocation and storage. In *International Conference on Green Communications and Networking* (Springer), 186–195

Gelenbe, E. (2012). Energy packet networks: adaptive energy management for the cloud. In *CloudCP'12: Proceedings of the 2nd International Workshop on Cloud Computing Platforms* (ACM, https://doi.org/10.1145/2168697.2168698), 1–5

[Dataset] Ikenaga, B. (2022, accessed on 12 February, 2022). Finite continued fractions, https://sites.millersville.edu/bikenaga/number-theory/finite-continued-fractions/finite-continued-fractions.html

Jones, G. L., Harrison, P. G., Harder, U., and Field, T. (2011). Fluid queue models of battery life. In *Proceeding of the 2011 IEEE 19th Annual International Symposium on Modelling, Analysis, and Simulation of Computer and Telecommunication Systems* (IEEE), 278–285. doi:10.1109/MASCOTS.2011.61

Kaj, I. and Konané, V. (2016). Modeling battery cells under discharge using kinetic and stochastic battery models. *Applied Mathematical Modelling* 40, 7901–7915

Kendall, D. G. (1953). Stochastic processes occurring in the theory of queues and their analysis by the method of the imbedded markov chain. *The Annals of Mathematical Statistics* 24, 338–354

Kleinrock, L. (1975). *Queueing Systems Vol. 1: Theory* (John Wiley & Sons)

Ku, M.-L., Chen, Y., and Liu, K. R. (2015). Data-driven stochastic models and policies for energy harvesting sensor communications. *IEEE Journal on Selected Areas in Communications* 33, 1505–1520

Kuaban, G. S., Czachórski, T., Gelenbe, E., Sharma, S., and Czekalski, P. (2023a). A markov model for a self-powered green iot device with state-dependent energy consumption. In *2023 4th International Conference on Communications, Information, Electronic and Energy Systems (CIEES)*. 1–7. doi:10.1109/CIEES58940.2023.10378778

Kuaban, G. S., Gelenbe, E., Czachórski, T., Czekalski, P., and Tangka, J. K. (2023b). Modelling of the energy depletion process and battery depletion attacks for battery-powered internet of things (iot) devices. *Sensors* 23

Kuzman, M., del Toro García, X., Escolar, S., Caruso, A., Chessa, S., and López, J. C. (2019). A testbed and an experimental public dataset for energy-harvested iot solutions. In *2019 IEEE 17th International Conference on Industrial Informatics (INDIN)* (IEEE), vol. 1, 869–876

Kwiatkowska, M., Norman, G., and Par, D. (2011). Prism 4.0: Verification of probabilistic real-time systems. In *Proc. 23rd International Conference on Computer Aided Verification (CAV'11)* (Springer), vol. LNCS 6806, 585–591

Lorentzen, L. and Waadeland, H. (1992). *Studies in Computation Mathematics 3* (Elsevier)

Massey, W. A., Ekwedike, E., Hempsher, R. C., and Pender, J. J. (2023). A transient symmetry analysis foe the m/m/1/k queue. *Queueing Systems* 103, 1–43

Miao, L., Huo, Z.-M., Rong, Y., Mu, H.-W., and Sun, Z.-X. (2023). Iot adaptive threshold energy management algorithm based on energy harvesting. *Ad Hoc Networks* 149, 103241

Morse, P. (1958). *Queues, Inventories and Maintenance* (Wiley)

Ng, D. W. K., Lo, E. S., and Schober, R. (2013). Energy-efficient resource allocation in ofdma systems with hybrid energy harvesting base station. *IEEE Transactions on Wireless Communications* 12, 3412–3427

Pecka, P., Nowak, M., Rataj, A., and Nowak, S. (2018). Solving large markov models described with standard programming language. *Communications in Computer and Information Science* 935, 57–67

Sadatdiynov, K., Cui, L., Zhang, L., Huang, J. Z., Salloum, S., and Mahmud, M. S. (2023). A review of optimization methods for computation offloading in edge computing networks. *Digital Communications and Networks* 9, 450–461

Sharma, O. P. and Gupta, U. (1982). Transient behaviour of an M/M/1/N Queue. *Stochastic Processing and Application* 13, 327–331

Stehfest, H. (1970). Numeric inversion of laplace transform. *Communication of ACM* 13, 47–49

Tákacs, L. (1962). *Introduction to the Theory of Queues* (Oxford University Press, London)

Tunc, C. and Akar, N. (2017). Markov fluid queue model of an energy harvesting IoT device with adaptive sensing. *Performance Evaluation* 111, 1–16

Varjovi, A. E. and Babaie, S. (2020). Green internet of things (giot): Vision, applications and research challenges. *Sustainable Computing: Informatics and Systems* 28, 100448

Waadeland, H. and Lorentzen, L. (2008). *Continued Fractions*, vol. 1 (Springer Science & Business Media)

Wang, H., Li, H., Wang, Z., Chen, X., and Ci, S. (2014). Stochastic queue modeling and key design metrics analysis for solar energy powered cellular networks. In *2014 International Conference on Computing, Networking and Communications (ICNC)* (IEEE), 472–477